Protein Science (1995), *4*:1305–1314. Cambridge University Press. Printed in the USA.

Interactions between hydrophobic side chains within α-helices

TREVOR P. CREAMER AND GEORGE D. ROSE

Department of Biophysics and Biophysical Chemistry, Johns Hopkins University School of Medicine, Baltimore, Maryland 21205

(RECEIVED March 10, 1995; ACCEPTED April 7, 1995)

Abstract

The thermodynamic basis of helix stability in peptides and proteins is a topic of considerable interest. Accordingly, we have computed the interactions between side chains of all hydrophobic residue pairs and selected triples in a model helix, using Boltzmann-weighted exhaustive modeling. Specifically, all possible pairs from the set Ala, Cys, His, Ile, Leu, Met, Phe, Trp, Tyr, and Val were modeled at spacings of $(i, i + 2)$, $(i, i + 3)$, and $(i, i + 4)$ in the central turn of a model poly-alanyl α-helix. Significant interactions—both stabilizing and destabilizing—were found to occur at spacings of $(i, i + 3)$ and $(i, i + 4)$, particularly in side chains with rings (i.e., Phe, Tyr, Trp, and His). In addition, modeling of leucine triples in a helix showed that the free energy can exceed the sum of pairwise interactions in certain cases. Our calculated interaction values both rationalize recent experimental data and provide previously unavailable estimates of the constituent energies and entropies of interaction.

Keywords: α-helix; hydrophobicity; protein conformation; protein folding; secondary structure

The α-helix was first proposed as a model structure by Pauling and co-workers (Pauling et al., 1951) and quickly confirmed in X-ray diffraction studies of Perutz (1951). Despite intense research during ensuing years, the thermodynamic basis of helix formation has only recently begun to emerge. Several groups have determined helix-propensity scales for the naturally occurring amino acids in peptides (Lyu et al., 1990, 1991; Merutka et al., 1990; O'Neil & DeGrado, 1990; Padmanabhan et al., 1990; Padmanabhan & Baldwin, 1991; Chakrabartty et al., 1994) and in proteins (Horovitz et al., 1992; Blaber et al., 1993). The rank order of helix propensities is similar in these scales, with values that are determined largely by differences in side-chain conformational entropy between the unfolded state and the helix (Creamer & Rose, 1992).

It has been proposed that, in addition to the intrinsic helical propensity of each residue, interactions between hydrophobic side chains within an α-helix can affect the stability of the structure (Lotan et al., 1966; Richards & Richmond, 1978; Dill et al., 1993). Such interactions are most likely to occur at intrahelical spacings of $(i, i + 3)$ and $(i, i + 4)$. In the first work to measure such interactions directly, Padmanabhan and Baldwin (1994a, 1994b) demonstrated the existence of stabilizing interactions of Leu with Ile, Leu, Phe, Tyr, and Val, where both members of each pair are near the center of a helical peptide.

In the present work, we calculate the interactions between all pairs of hydrophobic side chains spaced at $(i, i + 2)$, $(i, i + 3)$, and $(i, i + 4)$ in mid-helical positions. In detail, exhaustive conformational searching was used to calculate the interactions between all possible pairwise combinations of Ala, Cys, uncharged His, Ile, Leu, Met, Phe, Trp, Tyr, and Val at spacings of $(i, i + 2)$, $(i, i + 3)$, and $(i, i + 4)$ in the central turn of a model 19-residue poly-alanyl α-helix. Significant interactions were found to occur at spacings of $(i, i + 3)$ and $(i, i + 4)$, particularly in residue pairs where one of the side chains contains a ring (i.e., Phe, Tyr, Trp, and His). Both stabilizing and destabilizing interactions were seen. A preliminary study of the interactions between Leu and Phe side chains has been reported elsewhere (Creamer et al., 1995).

In addition, helical peptides containing three Leu residues at various spacings were modeled to assess the issue of pairwise additivity. In certain cases, the free energy of interaction exceeds that of the summed pairwise contributions.

Our calculated interaction energies are compared to the experimental results of Padmanabhan and Baldwin (1994a, 1994b), to the interaction tables of Muñoz and Serrano (1994), and to values derived from a dataset of helices in high-resolution protein structures.

Reprint requests to: George D. Rose, Department of Biophysics and Biophysical Chemistry, Johns Hopkins University School of Medicine, 725 N. Wolfe Street, Baltimore, Maryland 21205; e-mail: rose@grserv.med.jhu.edu.

Results

Modeled pairwise interaction energies

The calculated conformational energy and entropy between interacting pairs of guest residues at spacings of $(i, i + 3)$ and $(i, i + 4)$ in an α-helix, minus the corresponding values at $(i, i + 2)$, are listed in Tables 1 and 2, respectively. Estimated free energies of interaction, ΔA, are listed in Table 3. Notably, pairwise interactions are not symmetric; the value of pair (a, b) is not necessarily the same as that of (b, a) at the same spacing. For example, at a spacing of $(i, i + 4)$, the pair Met-Trp has an estimated interaction free energy, ΔA, of -0.56 kcal·mol^{-1}, whereas the pair Trp-Met has an interaction energy of -0.14 kcal·mol^{-1} (Table 3; Kinemage 1). Asymmetry is due to the fact that side chains in an α-helix are intrinsically directional; in a right-handed helix of L-amino acids, the β-carbons point toward the helix N-terminus.

The interaction between β-branched residues and ring-containing side chains also is order dependent. At a spacing of $(i, i + 4)$, there is a calculated net unfavorable free energy of 2 or 3 kcal·mol^{-1} between a β-branched residue at position i and a ring-bearing side chain at position $i + 4$ (Table 3). This effect is due to excluded volume constraints. β-Branched residues in helices favor the *trans* conformer (MacGregor et al., 1987), resulting in one of the γ-substituents pointing toward the helix C-terminus, and thus toward the residue at $i + 4$. When the $i + 4$ position is occupied by a large, inflexible side chain, such as a ring, a steric clash occurs. However, when the side-chain order is reversed, the free energy of interaction is near zero because in this case both side chains can occupy preferred conformations without steric overlap. The computed magnitude of the unfavorable free energy for a (β-branched, ring)-pair at $(i, i + 4)$ might be reduced were a smaller rotational increment used in the conformational search and/or nonrigid geometry employed.

The interaction between two ring-containing residues tends to be large and favorable at either spacing (Tables 1, 2; Kinemage 2). The two rings are capable of burying substantial surface area between them, resulting in a large, favorable conformational energy. In this case, the accompanying loss of side-chain entropy upon pairwise association is small because each bulky side chain has already lost most of its conformational entropy individually, upon helix formation. The only exceptions to this generalization involve the large, unfavorable interaction between a Trp at $i + 3$ and a ring-containing residue at i (Table 1), where the large Trp moiety cannot avoid a steric clash with another large group at position i.

At a spacing of $(i, i + 4)$, interactions between a bulky ring and a flexible side chain, such as Leu or Met, tend to be favorable in either orientation (Table 3). To a lesser extent, this generalization also holds true between a β-branched residue (Val or Ile) and a flexible side chain (Leu or Met). These interactions differ in that there is a relatively large loss of side-chain entropy

Table 1. *Calculated interaction energies and entropies for hydrophobic residues spaced at (i, i + 3) in a model helix normalized with respect to the same residues spaced at (i, i + 2)*[a]

	$i + 3$									
i	Ala	Cys	His	Ile	Leu	Met	Phe	Trp	Tyr	Val
Ala	0.00	0.01	0.01	0.01	0.02	0.01	0.02	0.01	0.01	−0.02
	0.00	0.00	0.00	0.00	0.00	0.00	0.00	0.00	0.00	0.00
Cys	0.02	0.00	−0.08	−0.03	−0.03	−0.09	−0.08	−0.37	−0.08	−0.04
	0.00	0.00	0.02	0.00	0.01	0.01	0.01	0.06	0.01	0.00
His	0.02	−0.03	−0.42	−0.15	−0.20	−0.34	−0.49	0.64	−0.52	−0.07
	0.00	0.00	0.17	0.01	0.04	0.07	0.10	−0.37	0.10	−0.01
Ile	0.02	−0.02	−0.23	−0.11	−0.15	−0.22	−0.26	−0.32	−0.27	−0.07
	0.00	0.00	0.04	0.01	0.02	0.03	0.03	0.17	0.03	0.00
Leu	0.02	−0.02	−0.27	−0.13	−0.19	−0.19	−0.32	0.30	−0.33	−0.07
	0.00	0.00	0.06	0.01	0.06	0.05	0.06	−0.21	0.06	−0.01
Met	0.02	−0.01	−0.18	−0.08	−0.11	−0.17	−0.22	−0.44	−0.23	−0.05
	0.00	0.00	0.02	0.01	0.01	0.06	0.02	0.09	0.02	−0.01
Phe	0.02	−0.03	−0.40	−0.16	−0.23	−0.34	−0.48	1.11	−0.50	−0.08
	0.00	0.00	0.10	0.02	0.05	0.08	0.12	−0.54	0.10	−0.01
Trp	0.02	−0.03	−0.38	−0.15	−0.22	−0.39	−0.46	1.11	−0.48	−0.07
	0.00	−0.01	0.00	−0.02	0.01	0.08	0.05	−0.42	0.03	−0.03
Tyr	0.02	−0.03	−0.40	−0.16	−0.23	−0.36	−0.49	1.01	−0.50	−0.08
	0.00	0.00	0.10	0.02	0.05	0.09	0.10	−0.47	0.11	0.00
Val	0.02	−0.01	−0.11	−0.05	−0.06	−0.16	−0.12	−0.48	−0.12	−0.05
	0.00	0.00	0.02	0.00	0.02	0.02	0.02	0.05	0.01	0.00

[a] For each entry, the top value is ΔE_{ab} and the bottom value is $-T\Delta S_{ab}$ (in kcal·mol^{-1}).

Table 2. *Calculated interaction energies and entropies for hydrophobic residues spaced at (i, i + 4) in a model helix normalized with respect to the same residues spaced at (i, i + 2)*[a]

	$i+4$									
i	Ala	Cys	His	Ile	Leu	Met	Phe	Trp	Tyr	Val
Ala	0.00	0.00	−0.01	0.06	0.00	−0.01	−0.01	−0.01	−0.01	0.00
	0.00	0.00	0.00	0.00	0.00	0.00	0.00	0.00	0.00	0.00
Cys	−0.01	−0.07	0.18	−0.10	−0.26	−0.09	0.04	−0.18	−0.07	−0.08
	0.00	0.01	−0.02	0.01	0.06	−0.02	0.13	0.29	0.21	0.00
His	−0.01	−0.01	−0.26	0.02	−0.32	−0.10	−0.35	−0.52	−0.47	0.03
	0.00	−0.08	0.05	−0.17	−0.07	−0.12	0.14	0.12	0.15	−0.13
Ile	−0.01	−0.14	1.49	−0.24	−0.44	−0.16	2.21	3.66	2.54	−0.17
	0.00	0.01	−0.36	0.01	0.09	0.00	−0.50	−0.72	−0.56	0.00
Leu	−0.01	−0.03	−0.27	0.00	−0.13	−0.15	−0.45	−0.81	−0.74	0.00
	0.00	−0.03	0.10	−0.09	0.11	−0.03	0.21	0.31	0.32	−0.06
Met	−0.01	−0.06	−0.30	−1.08	−0.29	−0.21	−0.51	−0.92	−0.50	−0.05
	0.00	−0.03	0.07	0.07	0.02	0.05	0.19	0.36	0.31	−0.05
Phe	−0.01	0.04	−0.26	0.14	−0.12	−0.04	−0.34	−0.54	−0.47	0.10
	0.00	−0.09	0.10	−0.21	−0.18	−0.14	0.07	0.12	0.15	−0.15
Trp	−0.01	0.04	−0.28	0.16	0.07	−0.03	−0.37	−0.72	−0.54	0.10
	0.00	−0.08	0.07	−0.22	−0.23	−0.11	0.08	0.10	0.09	−0.13
Tyr	−0.01	0.05	−0.25	0.17	−0.11	−0.02	−0.33	−0.53	−0.46	0.11
	0.00	−0.09	0.07	−0.25	−0.22	−0.18	0.11	0.10	0.10	−0.14
Val	−0.01	−0.12	1.52	−0.22	−0.39	−0.14	2.23	3.68	2.56	−0.15
	0.00	0.01	−0.40	0.00	0.08	−0.01	−0.51	−0.75	−0.56	0.00

[a] For each entry, the top value is ΔE_{ab} and the bottom value is $-T\Delta S_{ab}$ (in kcal·mol^{-1}).

between a ring and Leu or Met, whereas little entropy is lost between a β-branched group and Leu or Met. Individually, both rings and β-branched moieties have little conformational entropy to lose. Therefore, flexible side chains must be able to interact with a ring in multiple conformations. This conclusion is supported by the results of the conformational searches. As an example, the pair (Met, Phe) at a spacing of $(i, i+4)$ interacts in approximately 1,400 conformations, whereas the pair (Val, Phe) interacts in only 85 conformations. An interaction is said to occur in this case when the distance between any two atoms—one from each side chain—is closer than the sum of their respective van der Waals radii plus the diameter of a water molecule (2.8 Å).

Free energies of interaction at a spacing of $(i, i+4)$ are typically larger in magnitude (both favorable and unfavorable) than those at a spacing of $(i, i+3)$, but not always. For example, the Leu-Leu pair at $(i, i+3)$ has an estimated free energy of -0.13 kcal·mol^{-1}, whereas at $(i, i+4)$ the free energy of interaction is approximately zero. Two side chains are actually closer at $(i, i+3)$ than at $(i, i+4)$, with a distance between Cβ atoms of 5.7Å and 6.5Å, respectively. However, the vectors defined by the Cα–Cβ bonds of two side chains at $(i, i+4)$ are approximately parallel, whereas the corresponding vectors at $(i, i+3)$ are roughly orthogonal. Consequently, side-chain orientations at $(i, i+4)$ tend to promote interaction, whereas those at $(i, i+3)$ tend to inhibit interaction.

Side-chain conformational entropy makes an important contribution to the pairwise free energy of interaction, as illustrated in Tables 1 and 2. Indeed, in some cases interaction can result in a *gain* in conformational entropy—an observation that seems at first counterintuitive. For example, His-Trp at $(i, i+3)$ (Table 1) gains an estimated -0.37 kcal·mol^{-1} in entropy. A gain in entropy arises from a "flattening" of the distribution of side chains among their rotamer classes. Entropy is maximal when all rotamer classes are equally populated. In cases where a gain in entropy is observed, there is generally a concomitant large, unfavorable conformational energy term (+0.64 kcal·mol^{-1} in the His-Trp example) that "chases" the side chain out of otherwise favorable rotational minima and flattens the overall distribution.

Modeled triplet interaction energies

Results from conformational searches involving triplets of leucine residues are shown in Table 4. Leu (i) is positioned at residue 8 in the model helix, and the two digits in each peptide name indicate the spacing of the second and third residues. For example, peptide L26 has a pair of interacting leucine residues at $(i, i+2)$ and $(i, i+6)$.

The L28 peptide is used as a standard state because, at spacings of $(i, i+2, i+8)$, none of the leucines can interact. The Boltzmann-weighted distribution of rotamers obtained using this

Table 3. *Calculated free energy of interaction, $\Delta A_{ab} = \Delta E_{ab} - T\Delta S_{ab}$ (kcal·mol^{-1}), for hydrophobic residues spaced at (i, i + 3) and (i, i + 4) in a model helix normalized with respect to the same residues spaced at (i, i + 2)*[a]

	$i+3$ or $i+4$									
i	Ala	Cys	His	Ile	Leu	Met	Phe	Trp	Tyr	Val
Ala	0.00	0.01	0.01	0.01	0.03	0.01	0.02	0.01	0.02	−0.02
	0.00	0.00	−0.01	0.06	0.00	−0.01	−0.01	−0.01	−0.01	0.00
Cys	0.02	0.00	−0.06	−0.03	−0.02	−0.08	−0.07	−0.31	−0.07	−0.04
	−0.01	−0.06	0.16	−0.10	−0.20	−0.12	0.17	0.11	0.14	−0.08
His	0.02	−0.03	−0.25	−0.14	−0.16	−0.27	−0.39	0.28	−0.42	−0.09
	−0.01	−0.09	−0.21	−0.14	−0.40	−0.22	−0.20	−0.40	−0.31	−0.10
Ile	0.02	−0.02	−0.19	−0.10	−0.13	−0.19	−0.23	−0.15	−0.24	−0.07
	−0.01	−0.13	1.13	−0.23	−0.35	−0.16	1.71	2.94	1.98	−0.17
Leu	0.02	−0.02	−0.21	−0.12	−0.13	−0.15	−0.26	0.08	−0.27	−0.08
	−0.01	−0.06	−0.17	−0.09	−0.02	−0.17	−0.24	−0.51	−0.42	−0.06
Met	0.02	−0.02	−0.16	−0.09	−0.10	−0.11	−0.20	−0.35	−0.21	−0.07
	−0.01	−0.08	−0.23	−1.01	−0.27	−0.16	−0.32	−0.56	−0.19	−0.10
Phe	0.02	−0.03	−0.29	−0.14	−0.18	−0.26	−0.36	0.57	−0.41	−0.08
	−0.01	−0.05	−0.16	−0.08	−0.30	−0.19	−0.27	−0.41	−0.32	−0.04
Trp	0.02	−0.04	−0.37	−0.17	−0.21	−0.31	−0.41	0.69	−0.44	−0.10
	−0.01	−0.03	−0.22	−0.05	−0.16	−0.15	−0.29	−0.62	−0.46	−0.03
Tyr	0.02	−0.03	−0.30	−0.15	−0.18	−0.27	−0.39	0.54	−0.40	−0.09
	−0.01	−0.04	−0.17	−0.08	−0.33	−0.20	−0.22	−0.43	−0.36	−0.03
Val	0.02	0.01	−0.09	−0.05	−0.05	−0.14	−0.10	−0.43	−0.11	−0.05
	−0.01	−0.11	1.13	−0.21	−0.31	−0.15	1.72	2.93	2.00	−0.15

[a] In each cell, the top value is ΔA at $(i, i+3)$ and the bottom value is at $(i, i+4)$.

peptide are in close agreement with those from the standard state peptide with two leucines, used in pairwise calculations (data not shown).

The peptides L25 and L26 (Table 4) contain interacting Leu residues at spacings of $(i+2, i+5)$ and $(i+2, i+6)$, respectively. In each peptide, Leu (i) cannot interact with either of the other two Leu residues. Both peptides have interaction energy and entropy differences that are in reasonable agreement with their pairwise counterparts (Tables 1, 2). The L25 peptide has an interaction free energy of −0.22 kcal·mol^{-1}, lower than the $(i, i+3)$ Leu pair value of −0.13 kcal·mol^{-1} (Table 3). This difference may indicate interactions between the side chains at position i and $i+5$. The L26 peptide has an estimated free energy of −0.09 kcal·mol^{-1}, in close agreement with the −0.02 kcal·mol^{-1} obtained for the $(i, i+4)$ pair (Table 3).

A peptide with the three Leu residues spaced at $(i, i+1, i+2)$ (L12 in Table 4) was modeled to assess interactions between adjacent side chains. A few contacts between the side chains were found, and these result in a slightly favorable interaction energy and slightly increased side-chain conformational entropy (Table 4).

There are two classes of three-residue interactions involving $(i, i+3)$ and $(i, i+4)$ (Kinemages 3, 4). One is a clustered group, where the three residues are mutually interacting; the other is a distributed group, where the three residues form a "stripe" along one face of the helix. In both classes, the interaction energy is more favorable than that given by the summed pairwise constituents.

The clustered group has two possible permutations, which were modeled using peptides L14 and L34. L14 contains leucines spaced at $(i, i+1, i+4)$, and L34 contains leucines spaced at $(i, i+3, i+4)$. The two peptides are energetically similar (Table 4). Both cases have a large favorable interaction energy and a moderate entropy loss, resulting in a favorable free energy of interaction. In each case, the free energy of interaction is twice the sum of the pairwise interaction energies at $(i, i+3)$ and $(i, i+4)$ (Table 3). The side-chain entropy loss for either L14 or L34 approximates the summed pairwise entropy losses, but there is a net gain in interaction energy. In effect, both L14 and L34 pay the same "entropy price" as they would in simple pairwise interactions but realize improved side-chain to side-chain contacts, thereby amplifying the free energy.

Two possible permutations of the helical stripe were modeled using peptides L37 and L47. L37 contains leucines spaced at $(i, i+3, i+7)$, and L47 contains leucines spaced at $(i, i+4, i+7)$. In L37, the free energy of interaction is again amplified relative to the pairwise sums (Table 4). However, in this case amplification arises primarily because the triple loses less side-chain entropy than the sum of its constituent pairs, a consequence of more uniformly populated rotamer distributions. The L47 peptide has a free energy of interaction that is more than twice its summed pairwise constituents (Table 4), again a consequence

Table 4. *Calculated interactions between three Leu residues at various spacings within an α-helix*

Peptide	Spacings[a]	ΔE	$-T\Delta S$	ΔA
L12	$i+1, i+2$ $j+1$	−0.05	−0.07	−0.12
L28[b]	$i+2, i+8$ $j+6$	–	–	–
L25	$i+2, i+5$ $j+3$	−0.21	−0.01	−0.22
L26	$i+2, i+6$ $j+4$	−0.19	+0.10	−0.09
L14	$i+1, i+4$ $j+3$	−0.48	+0.19	−0.29
L34	$i+3, i+4$ $j+1$	−0.47	+0.15	−0.32
L37	$i+3, i+7$ $j+4$	−0.35	+0.11	−0.24
L47	$i+4, i+7$ $j+3$	−0.38	0.00	−0.38
L36	$i+3, i+6$ $j+3$	−0.43	−0.02	−0.45
L48	$i+4, i+8$ $j+4$	−0.35	+0.15	−0.20

[a] Position i is the eighth residue in the helix model. Position j is the position of the second of the guest hydrophobic residues. As an example, in the L12 peptide, $j = i + 1$.

[b] This peptide was used as the reference because the three leucine side chains cannot directly interact.

of the entropy term; in this case, there is no net loss in side-chain conformational entropy.

Two other triples that form a stripe were also modeled: L36 and L48 (Table 4). L36 contains two $(i, i+3)$ interactions, and L48 contains two $(i, i+4)$ interactions. In both cases, the interaction free energies are additive, being approximated by the sum of their two pairwise constituents. In L36, ΔA is equal to twice the ΔA of L25, which latter peptide has just the one $(i, i+3)$ interaction. Similarly, ΔA of L48 is nearly twice that of L26, which has one $(i, i+4)$ interaction. Furthermore, in both cases the constituent energies and entropies are individually additive (Tables 1, 2, 4).

Protein interactions

The free energies of interaction for helical hydrophobic residue pairs derived from a protein dataset are listed in Table 5, together with the corresponding calculated values from Table 3. Only well-populated pairs (i.e., 15 or more occurrences of the pair at both $(i, i+2)$ and either $(i, i+3)$ or $(i, i+4)$) with side chains larger than alanine were considered. Notably, with the exception of Val-Val, all pairs involve a Leu residue. After Ala, Leu is the next most abundant hydrophobic residue in protein helices.

Table 5. *Comparison of protein-derived free energies of interaction, ΔG_{ab}, with calculated $\Delta A_{ab} = \Delta E_{ab} - T\Delta S_{ab}$ (kcal·mol^{-1})*

$(i, i+3)$				$(i, i+4)$			
a	b	ΔG_{ab}	ΔA_{ab}	a	b	ΔG_{ab}	ΔA_{ab}
Ile	Leu	−0.26	−0.13	Ile	Leu	−0.39	−0.35
Leu	Ile	−0.43	−0.12	Leu	Ile	−0.47	−0.09
Leu	Leu	−0.35	−0.13	Leu	Leu	−0.40	−0.02
Leu	Val	−0.21	−0.08	Leu	Val	−0.19	−0.06
Phe	Leu	−0.15	−0.18	Phe	Leu	−0.10	−0.30
Val	Leu	−0.49	−0.05	Val	Leu	−0.54	−0.31
Val	Val	−0.17	−0.05	Val	Val	−0.28	−0.15

The correlation between protein-derived free energies and calculated free energies is poor (Table 5). In all cases in Table 5, the protein-derived free energies are favorable, whereas the calculated free energies range from near zero to favorable. Thus, the two sets differ in magnitude and, in particular, Leu-Leu pairs at both spacings have calculated free energies that are much smaller than their counterparts in protein helices.

Peptide interactions

Recently, Padmanabhan and Baldwin (1994a) measured the interactions between Tyr and Leu residues at spacings of $(i, i+3)$ and $(i, i+4)$ near the center of helical peptides. A comparison of their values from CD measurements and our calculated free energies of interaction is given in Table 6. There is good agreement between the two sets of data. The experimentally observed increase in helicity between pairs at $(i, i+3)$ and $(i, i+4)$ is reflected in the calculated free energies as well as the difference in helicity between Tyr-Leu and Leu-Tyr.

Padmanabhan and Baldwin (1994a) also measured the interactions between Tyr and Val residues. Here, there is poor agreement between the two sets of data. In the peptide, an increase in helicity was observed between Val at $i+3$ and at $i+4$, relative to Tyr at i. In the calculations for the corresponding peptides, there is a slight decrease in free energy for $(i, i+4)$ relative to $(i, i+3)$. However, we note that in Tyr-Val pairs, Tyr is the

Table 6. *Comparison with the CD measurements of peptides studied by Padmanabhan and Baldwin containing Leu and Tyr at interacting positions*

	Residues				
Peptide[a]	a	b	Spacing	$-[\theta]_{222}$[a]	ΔA_{ab}
3Y6L	Tyr	Leu	$i, i+3$	6,500 ± 100	−0.18
3Y7L			$i, i+4$	11,700 ± 300	−0.33
7L10Y	Leu	Tyr	$i, i+3$	10,500 ± 500	−0.27
6L10Y			$i, i+4$	13,600 ± 300	−0.42

[a] Taken from Padmanabhan and Baldwin (1994a).

initial residue in the peptide. Even without fraying, the first helical residue (i.e., Ncap) adopts backbone dihedral angles that depart from helical values, and consequently, these Tyr-Val pairs are not expected to have the same interaction energies that would be expected for identical pairs at mid-helical positions.

Padmanabhan and Baldwin (1994b) extended their measurements to include interactions between a number of additional hydrophobic pairs in helical peptides. All pairs studied involve a leucine residue. Experimental and calculated energies are compared in Table 7. The two data sets are in poor agreement when Leu is at position i (closer to the N-terminus of the peptide) and in good agreement when Leu is at position $i + 3$ and $i + 4$ (closer to the C-terminus of the peptide).

From NMR measurements of helical peptides, Muñoz and Serrano (1994) also derived interaction tables for side-chain pairs spaced at $(i, i + 3)$ and $(i, i + 4)$. With some exceptions, good agreement is found between the NMR-derived values for hydrophobic pairs and our calculated interactions, as shown in Figures 1 and 2.

At a spacing of $(i, i + 3)$, there are some pairs where Muñoz and Serrano observe a favorable interaction, whereas the calculated interaction is unfavorable (Fig. 1). Notably, all such discrepancies involve a bulky Trp residue at position $i + 3$ and either a ring-containing residue (i.e., His, Phe, Tyr, or Trp) or Leu at position i. In conformational searches, Trp clashes sterically with any bulky residue at position i; a favorable interaction is found only with either shorter (Cys, Ile, and Val) or more flexible (Met) residues. In their analysis, Muñoz and Serrano (1994) appear to have averaged over all ring-containing residues; $(i, i + 3)$ interactions between Trp and other residues are the same as those for Phe or Tyr. Possibly, unfavorable interactions involving Trp were submerged upon averaging. Muñoz and Serrano find only one unfavorable $(i, i + 3)$ interaction that we calculate to be favorable, viz., a His-His pair, presumably a result of electrostatic repulsion between protonated histidines.

A larger number of discrepancies is seen at a spacing of $(i, i + 4)$ (Fig. 2). There are a number of pairs that Muñoz and Serrano find with no interactions, but that we calculate to be somewhat favorable; all involve Leu or Met at i and a ring-containing res-

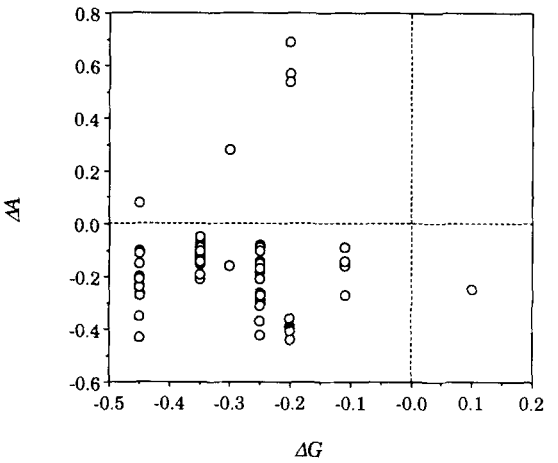

Fig. 1. Calculated interaction free energies plotted against interaction energies from Muñoz and Serrano (1994) for pairs of residues spaced at $(i, i + 3)$ in α-helices. Dashed lines represent free energies of 0.0 kcal·mol^{-1}. Points in the lower left quadrant are favorable in both the calculated table (Table 1) and the table of Muñoz and Serrano.

Table 7. *Comparison of pairwise interactions and summed pairwise interactions with the helical content of the peptides studied by Padmanabhan and Baldwin*

Residue pair[a]	Interactions	ΔA_{ab}[b]	ΔA_{sum}[c]	% Helix[d]
Leu-Leu	$i, i + 3$	−0.13	−0.54	68
	$i, i + 4$	−0.02	−0.39	76
Val-Leu	$i, i + 3$	−0.05	−0.28	52
	$i, i + 4$	−0.31	−0.51	68
Ile-Leu	$i, i + 3$	−0.13	−1.18	61
	$i, i + 4$	−0.35	−1.46	74
Phe-Leu	$i, i + 3$	−0.18	−0.64	44
	$i, i + 4$	−0.30	−0.72	58
Leu-Leu	$i, i + 3$	−0.13	−0.40	72
	$i, i + 4$	−0.02	−0.33	84
Leu-Val	$i, i + 3$	−0.08	−0.35	54
	$i, i + 4$	−0.06	−0.38	71
Leu-Ile	$i, i + 3$	−0.12	−0.38	71
	$i, i + 4$	−0.09	−0.39	84
Leu-Phe	$i, i + 3$	−0.26	−0.55	50
	$i, i + 4$	−0.24	−0.57	62

[a] Two sets of guest positions in the host peptide were used in the study by Padmanabhan and Baldwin (1994b): one for the (X-Leu) interactions and one for the (Leu-X) interactions. Consequently, there are two values for the (Leu-Leu) interaction.

[b] Pairwise free energies of interaction.

[c] Summed pairwise free energies of interaction as described in the text.

[d] Taken from Padmanabhan and Baldwin (1994b).

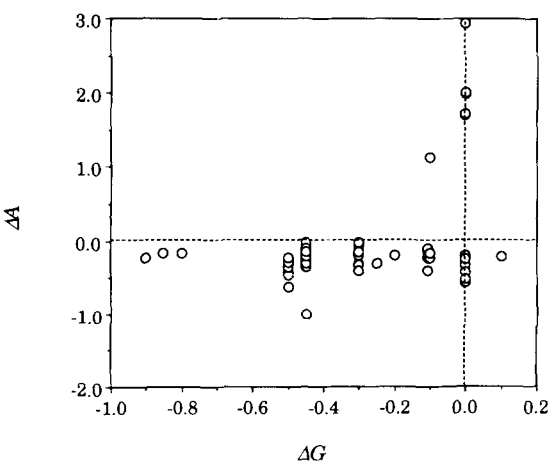

Fig. 2. Calculated interaction free energies plotted against interaction energies from Muñoz and Serrano (1994) for pairs of residues spaced at $(i, i + 4)$ in α-helices. Dashed lines represent free energies of 0.0 kcal·mol^{-1}. Points in the lower left quadrant are favorable in both the calculated table (Table 2) and the table of Muñoz and Serrano.

idue at $i + 4$. Conversely, eight interactions are calculated to be unfavorable but found by Muñoz and Serrano to be either favorable (two instances) or noninteracting (six instances). (Only four points are visible in Figure 2 because these eight points overlap.) In all instances, the residue at position i is Val or Ile, and the residue at $i + 4$ is a ring-containing residue. As described above, the calculations indicate steric clashes between β-branched residues and rings at these positions and orientations. Again, His-His is observed to be unfavorable by Muñoz and Serrano, whereas in calculations the pair is slightly favorable.

Discussion

We have modeled all pairwise interactions between hydrophobic side chains in α-helices in order to evaluate their contribution to helix stability. As seen (Tables 1, 2, 3; Kinemages 1–4), both stabilizing and destabilizing interactions are found at spacings of $(i, i + 3)$ and $(i, i + 4)$.

To some extent, these calculated values are model dependent, and possibly the use of a smaller rotational increment would have resulted in slightly different values for the interaction energies. However, the exhaustive calculations described here are very processor intensive, requiring many weeks on SGI Indigo 2 workstations, and a smaller increment would have been computationally prohibitive. Similarly, it might be thought that a model employing nonrigid geometry could lead to slightly different values through relaxation of sterically hindered structures. However, it has been shown that, after van der Waals radii have been scaled, the use of nonrigid geometry has little effect upon the calculated conformational behavior of isolated side chains in a model poly-alanyl helix (Creamer & Rose, 1994). A corresponding insensitivity to nonrigid geometry is expected in this work as well.

Our calculations employ a small hydrophobicity term of 4 cal·mol^{-1} Å^{-2} for exposed carbon group surface area (Wesson & Eisenberg, 1992). This term promotes burial of hydrophobic surface area between the two side chains and against the helix backbone. Neglecting this contribution leads to somewhat different side-chain rotamer distributions and consequently to differences in the calculated free energies of interaction. The side chains nonetheless still interact with one another due to favorable van der Waals interactions, the resulting interaction free energies being qualitatively very similar to those obtained using the hydrophobicity term (data not shown).

The calculated pairwise interactions were found to be order-dependent—(a, b) interaction values are not necessarily the same as (b, a) values at the same spacing (Tables 1, 2). This inescapable asymmetry results from the asymmetry of side-chain shapes together with the side-chain directionality that is inherent in α-helices.

Notable findings include large unfavorable interactions between β-branched side chains at i with ring-bearing residues at $i + 4$ (Table 2; Kinemage 1). These unfavorable interactions are simply an order-dependent steric incompatibility, and order reversal leads to favorable interactions. This steric incompatibility is reflected in the paucity of observed occurrences of these pairs in protein helices. In the data set of helices extracted from 120 high-resolution protein structures, the Ile-Trp pair appears only once at a spacing of $(i, i + 4)$, and the Val-Trp pair only seven times. Other interactions involving ring-bearing residues—notably those between two rings or a ring and a long flexible side chain—tend to be favorable (Tables 1, 2), a consequence of the large area buried by the ring and diminished entropy loss for ring-bearing side chains. This latter effect is due to the fact that the bulkier residues lose most of their conformational entropy individually, through interaction with the helical backbone (Creamer & Rose, 1992), leaving little further rotational freedom to lose in interactions with other residues.

The model peptides containing three interacting leucines (Kinemages 3, 4) demonstrate that, in general, pairwise interactions are nonadditive. In some triples, the free energy of interaction is enhanced with respect to the pairwise sums (peptides L14, L34, L37, and L47 in Table 4). Such enhancement is to be expected because, typically, a side chain will already have lost most if not all of its conformational entropy in pairwise interactions, with little or none remaining to lose in the triple. Nevertheless, the triple can provide the opportunity for improved side chain contacts, resulting in an enhanced free energy of interaction. Also, the side-chain entropy loss of a triple will be less than the summed entropy loss of its constituent pairs (see peptides L37 and L47 in Table 4) when rotamers in the triple are more uniformly populated than those in the pairs. Although the triplet free energy is well approximated by the summed pairwise interactions in two triples (peptides L36 and L48 in Table 4), pairwise additivity usually underestimates the magnitude of triplet interactions.

The calculated pairwise interaction energies do not agree well with free energies derived from the distributions observed in proteins (Table 5). Although both calculated and protein-derived interactions are favorable, neither the rank order nor the magnitude of the interactions agree. These discrepancies are hardly surprising. Hydrophobic residues in protein helices are typically situated within the protein core, where they can be far better buried than in a peptide. Additionally, higher order interactions can also play a more significant role in the heterogeneous background of a protein than in a poly-alanyl-helix.

The calculated free energies agree well with the Leu-Tyr interactions measured by Padmanabhan and Baldwin (1994a), as seen in Table 6. The increase in measured helicity from a spacing of $(i, i + 3)$ to $(i, i + 4)$ is also observed in the calculated free energies. Similarly, differences between the measured helicities of Leu-Tyr and Tyr-Leu are reflected in the calculations.

With the exception of Leu-Leu, experimental (Padmanabhan & Baldwin, 1994b) and calculated results agree for X-Leu pairs but disagree for Leu-X pairs (X = Leu, Val, Ile, and Phe) (Table 7). A possible reason for the discrepancy involves lysine residues, which may interact with the hydrophobic pair under assessment in the Padmanabhan and Baldwin peptides. Such interactions are not unlikely because lysine side chains have substantial hydrophobic surface and are flexible. The sequences and putative interactions in these peptides are illustrated in Figure 3.

A rough estimate of the total interaction free energies, ΔA_{sum}, in the Padmanabhan and Baldwin (1994b) peptides can be made by using methionine to approximate the aliphatic moiety in the lysine side chain and assuming pairwise additivity. Such estimates are given in Table 7. With the exception of Leu-Leu interactions, the summed pairwise interactions still give good agreement with the experimental results for X-Leu interactions. Although the agreement between ΔA_{sum} and the experimental results for the Leu-X pairs is still not good, it is much improved relative to the pairwise free energies. In all cases other than Leu-Leu, the estimated Leu-X free energies are the same for spac-

Ia : X - L (*i,i+3*) interactions

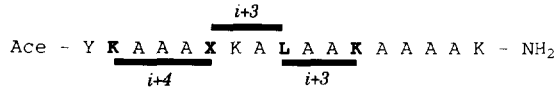

Ib : X - L (*i,i+4*) interactions

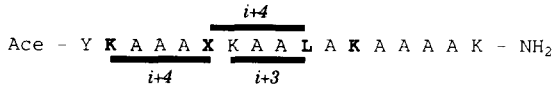

IIa : L - X (*i,i+3*) interactions

IIb : L - X (*i,i+4*) interactions

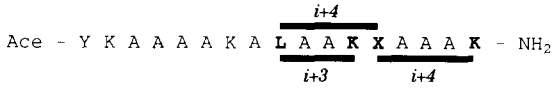

Fig. 3. Host peptides used by Padmanabhan and Baldwin (1994b), with putative pairwise interactions between side chains annotated by solid bars. The interacting leucine and X residues and the lysines that may also interact are denoted in bold type.

ings of (i, $i + 3$) and (i, $i + 4$), in contrast to the experimental results where the (i, $i + 4$) spacing results in greater helicity.

In Figure 4, computed differences in helicity between the summed pairwise free energies at spacings of (i, $i + 4$) and (i, $i + 3$), $\Delta\Delta A_{sum}$, are plotted against corresponding measured differences, Δ(% Helix). The measured differences spans a narrow range, from 8% to a maximum of 17%. Notably, the two Leu-Leu pairs have values of $\Delta\Delta A_{sum} < 0.0$ kcal·mol^{-1} (Fig. 4), indicating that the (i, $i + 3$) spacing is calculated to be more favorable than (i, $i + 4$) (Table 3). As noted above, pairwise interactions are often not additive and can underestimate the free energy of higher-order interactions, such as those in the Padmanabhan and Baldwin peptides (Fig. 3).

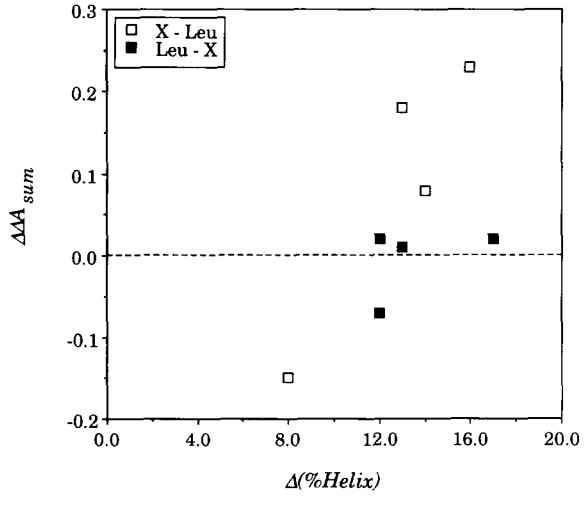

Fig. 4. Difference in helicity between the (i, $i + 4$) and (i, $i + 3$) pairs measured by Padmanabhan and Baldwin (1994b) plotted against the difference in summed pairwise free energies of interaction. Dashed line represents a difference in free energy of 0.0 kcal·mol^{-1}. X-Leu pairs are shown as open squares, and Leu-X pairs are plotted as filled squares. The two points with $\Delta\Delta A_{sum} < 0.0$ are the two Leu-Leu pairs, and their negative values indicate that the (i, $i + 3$) spacing is calculated to be more favorable than (i, $i + 4$), whereas the converse result is found experimentally.

It should be noted that the peptides used by Padmanabhan and Baldwin (1994a) to assess Leu-Tyr interactions also contain lysines that can interact with the leucine and/or tyrosine. After substituting methionine for lysine as above, the calculated ΔA_{sum} values are in close agreement with experimental values (data not shown).

Overall agreement is found between the NMR-derived interaction energies of Muñoz and Serrano (1994) and our calculated interaction free energies (Figs. 1, 2). To obtain sufficient data, Muñoz and Serrano pooled their results for similar side chains. For example, the ring-bearing residues—Phe, Trp, and Tyr—were considered as a group. In contrast, each residue was treated separately in our work, with results that differ in detail from those of Muñoz and Serrano (1994). Nonetheless, the majority of pairs found to be favorable by Muñoz and Serrano are also observed to be favorable in our work. This can be seen in Figures 1 and 2: most points cluster in the lower left quadrant of the plots.

The interaction tables provided here should prove useful in both experimental and theoretical studies of peptide and protein α-helices. Free energies were derived under the assumption of prior helicity and do not include contributions from intrinsic helix propensities (Creamer & Rose, 1992, 1994). Side-chain interaction energies range from stabilizing to destabilizing, with magnitudes that vary widely. These energies depend upon both individual residue characteristics (i.e., shape, polarity, conformational flexibility) and local environment (i.e., the nature and spacings of surrounding residues). The detailed analysis of helix stability would require that such factors be included.

Methods

Pairwise interaction energies

A 19-residue model polyalanyl α-helix was used in these studies, with N- and C-termini acetylated and methyl-amidated, respectively. The 19-residue model is long enough to avoid interactions between side chains of interest and the helix termini. Side chain pairs were situated at spacings of (i, $i + 2$), (i, $i + 3$), and (i, $i + 4$), where i is the 8th residue of the helix in all cases. Ten hydrophobic residues—viz., Ala, Cys, uncharged His, Ile, Leu, Met, Phe, Trp, Tyr, and Val—were modeled in all possible pairwise combinations at each spacing.

Pairwise interactions between side chains were reckoned in an exhaustive conformational search, with the energy sampled at each step. Starting from the all-*trans* configuration, side-chain torsion angles, χ_i, were searched in increments of 30°, with the exception of Met χ_3, which was searched in increments of 120°, and the hydroxyl hydrogen of Tyr, which was searched in increments of 180°. Both backbone and side-chain bond lengths and angles were held rigid.

Energy was calculated using the AMBER/OPLS forcefield (Weiner et al., 1984; Jorgensen & Tirado-Rives, 1988) at a tem-

perature of 298 K and a dielectric of bulk water, $\epsilon = 78$. This forcefield uses a united atoms approximation in which nonpolar hydrogens are not represented explicitly; instead, the van der Waals radii of parent atoms are expanded appropriately. In our work, the radii of united atoms (i.e., CH, CH_2, and CH_3 groups) were scaled to 90% of their van der Waals radii. With such scaling, the rotamer distributions of hydrophobic residues in a rigid helix reproduce those observed in protein helices (Creamer & Rose, 1992, 1994).

A factor of 4 cal·mol^{-1} Å^{-2}, from the solvation model of Wesson and Eisenberg (1992), was utilized for a polar surface exposed to solvent. This term favors the burial of hydrophobic surfaces. Surface area calculations were performed using the algorithm of Richmond (1984).

The Boltzmann-averaged conformational energy for a pair of residues (a, b) is calculated from

$$\langle E_{ab} \rangle = \sum_i^N E_i p_i, \tag{1}$$

where the sum is taken over all N conformations, E_i is the energy of the ith conformation, and p_i is the Boltzmann weighting factor. The weighting factors are calculated from the partition function for that pair of residues:

$$p_i = \frac{e^{-E_i/RT}}{Q}, \tag{2}$$

where R is the gas constant and T is the temperature (298 K). The partition function, Q, is calculated as

$$Q = \sum_k^N e^{-E_k/RT}. \tag{3}$$

Side-chain conformational entropy for a pair of side chains is given by

$$S_{ab} = -R \sum_i^N p_i \ln p_i, \tag{4}$$

where the sum is taken over all conformations.

For a pair of side chains (a, b), the "free energy of interaction," ΔA_{ab}, is given by the difference between the energy and entropy at either (i, $i + 3$) or (i, $i + 4$) and the energy and entropy at (i, $i + 2$):

$$\Delta A_{ab} = \Delta E_{ab} - T\Delta S_{ab}. \tag{5}$$

The pair at (i, $i + 2$) is used as the reference state because, at this spacing, the two side chains are situated on opposite sides of the helix where they cannot interact directly.

Triples of leucine residues

To assess the additivity of pairwise interaction energies, interactions between three leucines at various spacings were modeled by exhaustive conformational search. Free energies of interaction were calculated as above.

Protein side-chain interaction energies

A database of 127 unique chains from 120 high-resolution protein structures (i.e., R-factor ≤20%; resolution ≤2.0Å) from the Brookhaven Protein Data Bank (PDB) (Bernstein et al., 1977) was chosen from a set compiled by Hobohm et al. (1992). Within this set, each chain is less than 30% identical in sequence to any other. Proteins, specified by their four-letter PDB identifiers, include: 1aap, 1aba, 1abh, 1abk, 1ads, 1aoz, 1arb, 1ayh, 1bab, 1bbh, 1bbp, 1bgc, 1bop, 1btc, 1caj, 1cbn, 1cmb, 1cob, 1cox, 1cpc, 1cse, 1dfn, 1dri, 1eco, 1end, 1ezm, 1fas, 1fba, 1fcs, 1fdd, 1fia, 1gky, 1gmp, 1gox, 1gpb, 1hil, 1hiv, 1hle, 1hsb, 1ifc, 1isu, 1l92, 1lts, 1mdc, 1nxb, 1ofv, 1omp, 1osa, 1paz, 1pda, 1phb, 1poa, 1poc, 1ppb, 1ppf, 1ppn, 1rbp, 1rnd, 1rro, 1s01, 1sbp, 1sgt, 1sha, 1shf, 1smr, 1snc, 1ten, 1tfg, 1tgs, 1trb, 1tro, 1ttb, 1utg, 1ycc, 256b, 2aza, 2ccy, 2cdv, 2cpl, 2ctc, 2cts, 2cyp, 2er7, 2had, 2hpd, 2ihl, 2lal, 2mhr, 2mnr, 2msb, 2pia, 2por, 2rn2, 2scp, 2sga, 2sn3, 2zta, 3b5c, 3cbh, 3chy, 3cla, 3dfr, 3grs, 3il8, 3rub, 3sgb, 3sic, 4blm, 4enl, 4fxn, 4gcr, 4ins, 5p21, 7aat, 8abp, 8acn, 8rxn, 9ldt, 9rnt, and 9wga.

All α-helices of seven residues or more in length were extracted from the protein data set. Helices were identified using the criteria of Presta and Rose (1988) and were chosen to include residues N1 through C1 (viz., all residues having both helical backbone dihedral angles and helical hydrogen bonding); Ncap and Ccap residues were not included. The number of occurrences of each pair of hydrophobic residues at spacings of (i, $i + 2$), (i, $i + 3$), and (i, $i + 4$) was counted. Pairwise free energies of interaction for residues (a, b) at spacings of (i, $i + 3$) and (i, $i + 4$) were estimated from

$$\Delta G_{ab} = -RT \ln \frac{\text{no. occurrences of } (a, b) \text{ at } (i, i + n)}{\text{no. occurrences of } (a, b) \text{ at } (i, i + 2)}, \tag{6}$$

where $n = 3$ or 4.

Acknowledgments

We thank Rajeev Aurora and Rajgopal Srinivasan for enlightening discussions and critical reading of the manuscript and Robert Baldwin for providing copies of manuscripts prior to publication. This work was supported by NIH grant GM 29458.

References

Bernstein FC, Koetzle TF, Williams GJB, Meyer EF Jr, Brice MD, Rodgers JR, Kennard O, Shimanouchi T, Tasumi M. 1977. The Protein Data Bank: A computer-based archival file for macromolecular structures. *J Mol Biol 112*:535–542.

Blaber M, Zhang XJ, Matthews BW. 1993. Structural basis of amino acid α helix propensity. *Science 260*:1637–1640.

Chakrabartty A, Kortemme T, Baldwin RL. 1994. Helix propensities of the amino acids measured in alanine-based peptides without helix-stabilizing side-chain interactions. *Protein Sci 3*:843–852.

Creamer TP, Rose GD. 1992. Side-chain entropy opposes α-helix formation but rationalizes experimentally determined helix-forming propensities. *Proc Natl Acad Sci USA 89*:5937–5941.

Creamer TP, Rose GD. 1994. α-Helix-forming propensities in peptides and proteins. *Proteins Struct Funct Genet 19*:85–97.

Creamer TP, Srinivasan R, Rose GD. 1995. Evaluation of interactions between residues in α-helices by exhaustive conformational search. *Techniques Protein Chem VI*:443–450.

Dill KA, Fiebig KM, Chan HS. 1993. Cooperativity in protein-folding kinetics. *Proc Natl Acad Sci USA 90*:1942–1946.

Hobohm U, Scharf M, Schneider R, Sander C. 1992. Selection of representative protein data sets. *Protein Sci 1*:409–417.

Horovitz A, Matthews JM, Fersht AR. 1992. α-Helix stability in proteins. II. Factors that influence stability at an internal position. *J Mol Biol 227*:560–568.

Jorgensen WL, Tirado-Rives J. 1988. The OPLS potential function for proteins. Energy minimizations for crystals of cyclic peptides and crambin. *J Am Chem Soc 110*:1657–1666.

Lotan N, Yaron A, Berger A. 1966. The stabilization of the α-helix in aqueous solution by hydrophobic side chain interaction. *Biopolymers 4*:365–368.

Lyu PC, Liff MI, Marky LA, Kallenbach NR. 1990. Side chain contributions to the stability of alpha-helical structure in peptides. *Science 250*: 669–673.

Lyu PC, Sherman JC, Chen A, Kallenbach NR. 1991. α-Helix stabilization by natural and unnatural amino acids with alkyl side chains. *Proc Natl Acad Sci USA 88*:5317–5320.

MacGregor MJ, Islam SA, Sternberg MJE. 1987. Analysis of the relationship between side-chain conformation and secondary structure in globular proteins. *J Mol Biol 198*:295–310.

Merutka G, Lipton W, Shalongo W, Park SH, Stellwagen E. 1990. Effect of central-residue replacements on the helical stability of a monomeric peptide. *Biochemistry 29*:7511–7515.

Muñoz V, Serrano L. 1994. Elucidating the folding problem of helical peptides using empirical parameters. *Nature Struct Biol 1*:399–409.

O'Neil KF, DeGrado WF. 1990. A thermodynamic scale for the helix-forming tendencies of the commonly occurring amino acids. *Science 250*:646–652.

Padmanabhan S, Baldwin RL. 1991. Straight-chain non-polar amino acids are good helix-formers in water. *J Mol Biol 219*:135–137.

Padmanabhan S, Baldwin RL. 1994a. Helix-stabilizing interaction between tyrosine and leucine or valine when the spacing is *i*, *i* + 4. *J Mol Biol 241*:706–713.

Padmanabhan S, Baldwin RL. 1994b. Tests for helix-stabilizing interactions between various nonpolar side chains in alanine-based peptides. *Protein Sci 3*:1992–1997.

Padmanabhan S, Marqusee S, Ridgeway T, Laue TM, Baldwin RL. 1990. Relative helix-forming tendencies of nonpolar amino acids. *Nature (Lond) 344*:268–270.

Pauling L, Corey RB, Branson HR. 1951. The structures of proteins: Two hydrogen-bonded helical configurations of the polypeptide chain. *Proc Natl Acad Sci USA 37*:205–210.

Perutz MF. 1951. New X-evidence on the configuration of polypeptide chains. *Nature (Lond) 167*:1053–1054.

Presta LG, Rose GD. 1988. Helix signals in proteins. *Science 240*:1632–1641.

Richards FM, Richmond T. 1978. Solvent, interfaces and protein structure. *CIBA Found Symp 60*:23–45.

Richmond TJ. 1984. Solvent accessible surface area and excluded volume in proteins. Analytical equations for overlapping spheres and implications for the hydrophobic effect. *J Mol Biol 178*:63–89.

Weiner SJ, Kollman PA, Case DA, Singh UC, Ghio C, Alagona G, Profeta S Jr, Weiner P. 1984. A new force field for molecular mechanical simulation of nucleic acids and proteins. *J Am Chem Soc 106*:765–784.

Wesson L, Eisenberg D. 1992. Atomic solvation parameters applied to molecular dynamics of proteins in solution. *Protein Sci 1*:227–235.